Neutron stars in the derivative coupling model

N. K. Glendenning and F. Weber
Nuclear Science Division, Lawrence Berkeley Laboratory, University of California, One Cyclotron Road, Berkeley, California 94720

S. A. Moszkowski
University of California at Los Angeles, Department of Physics, Los Angeles, California 90024

(Received 13 May 1991)

Properties of neutron stars derived from the hybrid derivative coupling model of nuclear field theory are studied. Generalized beta equilibrium with all baryon types to convergence is allowed. Hyperon couplings compatible with the inferred binding energy of the lambda hyperon in saturated nuclear matter predict a large hyperon population, with neutrons having a bare majority population in a $1.5M_{\odot}$ neutron star. Among the properties studied are the limits on rotation imposed by gravitation-radiation-reaction instabilities as moderated by viscosity. These instabilities place a lower limit on rotational periods of neutron and hybrid stars of about 1 ms.

PACS number(s): 21.65.+f, 21.80.+a, 97.60.Jd, 12.38.Mh

I. INTRODUCTION

In this paper we study a broad range of properties of neutron stars derived from a variant of the derivative coupling nuclear field theory that was recently shown to economically describe the bulk properties of nuclear matter [1]. Relativistic field theories of nuclear matter and finite nuclei have enjoyed a renaissance in recent years, and they have the virtue of describing nuclear matter at saturation, many features of finite nuclei, both spherical and deformed, and they extrapolate causally to high density.

The σ-ω nuclear field theory has been broadly studied in both spherical and deformed nuclei. However, in the linear version [2] it has too small a nucleon effective mass ($\sim 0.55 m_N$) at saturation density of nuclear matter and too large a compression modulus (~ 560 MeV). These properties can be brought under control at the cost of two additional parameters by the addition of scalar cubic and quartic self-interactions in the so-called nonlinear model [3]. Alternatively, it has been recently noticed by Zimanyi and Moszkowski [1] that, if the scalar field is coupled to the derivative of the nucleon field, these two nuclear properties are automatically in reasonable accord with present knowledge of their values, the two coupling constants of the theory being fixed by the empirical saturation density and binding as in the linear σ-ω theory. The agreement with bulk nuclear properties can be further improved by a slight modification of the model of Zimanyi and Moszkowski, which we shall call the hybrid derivative coupling model, and which we discuss below. Renormalization is irrevocably lost in derivative coupling models, but since (strong interacting) nuclear field theory is usually regarded as an effective one, this does not seem to be a weighty objection. Since, in the derivative coupling model, only two coupling constants are needed to reproduce four nuclear properties (ρ_0, B/A, m^*, K), it is interesting to explore its predictions for neutron star properties. This we do for a wider range of properties than is usual. For example, we calculate the general relativistic Kepler frequency for the family of stars and the gravity-wave instabilities as moderated by viscosity. In addition, we discuss the connection of the Λ hyperon binding as inferred from measurements of energy levels in hypernuclei, and the coupling constants of the theory. We find, unlike earlier works [4–6], that the coupling in the two systems, hypernuclei and neutron stars, *can* be made consistent. Altogether, the model accounts for the bulk nuclear properties, ρ_0, B/A, m^*, K, $a_{\rm sym}$, and the Λ binding $(B/A)_{\Lambda}$.

Neutron stars are not pure in neutrons, as their name might imply. The lowest-energy state of cold, charge neutral matter is not pure neutron matter, but matter that is in beta equilibrium. At the high densities that may be present in the cores of the most massive neutron stars, this equilibrium will involve not only the neutron, proton, and leptons, but also such higher mass baryons for which the baryon chemical potential exceeds their mass (corrected for interactions and electric charge). We need, therefore, to generalize the Lagrangian for nuclear matter analogous to the way the earlier theories were generalized [7,8].

II. HYBRID DERIVATIVE COUPLING NUCLEAR FIELD THEORY

In place of the purely derivative coupling of the scalar field to the baryons and vector meson of the Zimanyi-Moszkowski model, we couple it here by both Yukawa point and derivative coupling to baryons and both vector fields. This improves the agreement with the compression modulus and effective nucleon mass at saturation. The nuclear matter properties are quoted later. To account for the symmetry force, we include the coupling of the rho meson to the isospin current. The rho meson contribution to this current vanishes in the mean-field approximation and so we do not write its formal contribution in the Lagrangian [9]:

$$\mathcal{L}=\sum_B \left[\left[1+\frac{g_{\sigma B}\sigma}{2m_B}\right] [\bar{\psi}_B(i\gamma_\mu\partial^\mu - g_{\omega B}\gamma_\mu\omega^\mu - \tfrac{1}{2}g_{\rho B}\gamma\tau\cdot\rho^\mu)\psi_B] - \left[1-\frac{g_{\sigma B}\sigma}{2m_B}\right] m_B\bar{\psi}_B\psi_B \right]$$
$$+\tfrac{1}{2}(\partial_\mu\sigma\partial^\mu\sigma - m_\sigma^2\sigma^2) - \tfrac{1}{4}\omega_{\mu\nu}\omega^{\mu\nu} + \tfrac{1}{2}m_\omega^2\omega_\mu\omega^\mu - \tfrac{1}{4}\rho_{\mu\nu}\cdot\rho^{\mu\nu} + \tfrac{1}{2}m_\rho^2\rho_\mu\cdot\rho^\mu + \sum_\lambda \bar{\psi}_\lambda(i\gamma_\mu\partial^\mu - m_\lambda)\psi_\lambda . \quad (1)$$

In the first term one sees the coupling of the scalar field to the derivatives of the baryon fields and to the vector mesons. The Yukawa point coupling to the baryon fields is contained in the second term. In the last line one recognizes the free scalar, vector, vector-isovector mesons, and lepton Lagrangians. The latter must be present because of charge neutrality. (We use the notation $\omega_{\mu\nu}=\partial_\mu\omega_\nu-\partial_\nu\omega_\mu$ and other conventions of Ref. [10].) The baryon Lagrangian is in the first line together with the interaction terms with the above-mentioned mesons. The ρ-mesons coupling constant will be adjusted to give the empirical symmetry coefficient. The sum on B is extended over all baryons including their charge states to convergence, of which the most obvious are listed in Table I. The solution is most easily obtained by means of the transformation of all baryon fields by

$$\psi_B=\left[1+\frac{g_{\sigma B}\sigma}{2m_B}\right]^{-1/2}\Psi_B . \quad (2)$$

The equivalent Lagrangian is

$$\mathcal{L}=\sum_B \bar{\Psi}_B(i\gamma_\mu\partial^\mu - m_B^* - g_{\omega B}\gamma_\mu\omega^\mu - \tfrac{1}{2}g_{\rho B}\gamma_\mu\tau\cdot\rho^\mu)\Psi_B$$
$$+\tfrac{1}{2}(\partial_\mu\sigma\partial^\mu\sigma - m_\sigma^2\sigma^2) - \tfrac{1}{4}\omega_{\mu\nu}\omega^{\mu\nu} + \tfrac{1}{2}m_\omega^2\omega_\mu\omega^\mu$$
$$-\tfrac{1}{4}\rho_{\mu\nu}\cdot\rho^{\mu\nu} + \tfrac{1}{2}m_\rho^2\rho_\mu\cdot\rho^\mu + \sum_\lambda \bar{\psi}_\lambda(i\gamma_\mu\partial^\mu - m_\lambda)\psi_\lambda . \quad (3)$$

It is evident that the baryons now have effective masses,

$$m_B^*=\left[1-\frac{g_{\sigma B}\sigma}{2m_B}\right]\left[1+\frac{g_{\sigma B}\sigma}{2m_B}\right]^{-1} m_B . \quad (4)$$

We solve the field equations in the frequently used mean-field approximation (Hartree) [11]. In this approximation, the theory is regarded as an effective one in which coupling constants are adjusted to properties of nuclear matter or finite nuclei, but not to the vacuum interaction between nucleons. The baryon source currents in the Euler-Lagrange equations for the mesons are replaced by their ground-state expectation values. The ground state is defined as having the single-particle momentum eigenstates of the Dirac equations filled to the top of the Fermi sea for each baryon species in accord with the conditions of chemical equilibrium. We describe how this is done below.

The meson-field equations in uniform static matter, in which space and time derivatives can be dropped, are

$$\omega_0=\sum_B \frac{g_{\omega B}}{m_\omega^2} n_B , \quad (5)$$

$$\rho_{03}=\sum_B \frac{g_{\rho B}}{m_\rho^2} I_{3B} n_B , \quad (6)$$

$$m_\sigma^2\sigma=\sum_B g_{\sigma B}\left[1+\frac{g_{\sigma B}\sigma}{2m_B}\right]^{-2}\langle\bar{\Psi}_B\Psi_B\rangle$$
$$=\sum_B g_{\sigma B}\left[1+\frac{g_{\sigma B}\sigma}{2m_B}\right]^{-2}\frac{2J_B+1}{2\pi^2}$$
$$\times\int_0^{k_B}\frac{m_B^*}{\sqrt{k^2+m_B^{*2}}}k^2dk . \quad (7)$$

The bracket $\langle \cdots \rangle$ denotes ground-state expectation. A simple way of computing such expectation values without the need of constructing the Dirac spinors is described in

TABLE I. Baryons and their charge states. Spin is J, isospin is I, its third component I_3, charge is q, and strangeness is s.

	m (MeV)	J	I	I_3	q	s
N	939	$\frac{1}{2}$	$\frac{1}{2}$	$-\frac{1}{2}$	0	0
				$\frac{1}{2}$	1	0
Δ	1232	$\frac{3}{2}$	$\frac{3}{2}$	$-\frac{3}{2}$	-1	0
				$-\frac{1}{2}$	0	
				$\frac{1}{2}$	1	
				$\frac{3}{2}$	2	
Λ	1115	$\frac{1}{2}$	0	0	0	-1
Σ	1190	$\frac{1}{2}$	1	-1	-1	-1
				0	0	
				1	1	
Ξ	1315	$\frac{1}{2}$	$\frac{1}{2}$	$-\frac{1}{2}$	-1	-2
				$\frac{1}{2}$	0	
Ω	1673	$\frac{3}{2}$	0	0	-1	-3

Ref. [8]. The spacelike components of both vector fields vanish as can be shown explicitly [8]; they do so for the physical reasons that the ground state is isotropic and has definite charge.

The condition of charge neutrality is expressed by

$$q_H + q_e = 0 ,$$
$$q_H \equiv \sum_B (2J_B+1) q_B k_B^3/(6\pi^2) , \tag{8}$$
$$q_e \equiv -\sum_\lambda k_\lambda^3/(3\pi^2) = 0 ,$$

where the first sum is over the baryons whose electric charges are denoted by q_B, Fermi momenta by k_B, and the second sum is over the leptons e^- and μ^-.

Chemical equilibrium can be imposed through the two independent chemical potentials, μ_n, μ_e, for the conserved baryon and (negative) electron charge. Strangeness is not conserved on any macroscopic time scale. For the baryon species, B, we have $\mu_B = \mu_n - q_B \mu_e$. The Fermi momenta for the baryons are the positive real solutions of

$$\mu_B = e_B(k_B) \quad (N \text{ equations}) , \tag{9}$$

where N is the number of different baryon species including their charge states that are listed in Table I, and the Dirac eigenvalues $e_B(k)$ are defined below. The lepton Fermi momenta are the positive real solutions of

$$\sqrt{k_e^2 + m_e^2} = \mu_e , \tag{10}$$
$$\sqrt{k_\mu^2 + m_\mu^2} = \mu_\mu = \mu_e . \tag{11}$$

At a chosen baryon density

$$\rho = \sum_B n_B , \tag{12}$$
$$n_B \equiv \langle \Psi_B^\dagger \Psi_B \rangle = (2J_B+1) k_B^3/(6\pi^2) , \tag{13}$$

the solution of the above coupled equations (5)–(12) provides the values for

$$\sigma, \omega_0, \rho_{03}, \mu_n, \mu_e, k_e, k_\mu, k_n, k_p, k_\Lambda, \ldots \tag{14}$$

of which there are $(7+N)$.

The Dirac equations for the baryons are

$$(i\gamma_\mu \partial^\mu - m_B^* - g_{\omega B}\gamma_\mu \omega^\mu - \tfrac{1}{2} g_{\rho B} \gamma_\mu \tau \cdot \rho^\mu)\Psi_B = 0 . \tag{15}$$

Taking account of the vanishing of the spacelike components of the vector fields, the eigenvalues can be found as

$$e_B(k) = g_{\omega B}\omega_0 + g_{\rho B}\rho_{03} I_{3B} + \sqrt{k^2 + m_B^{*2}} . \tag{16}$$

In the above equations, I_{3B} is the isospin projection of baryon charge state B. This completes a description of the equations that define the solution of the above Lagrangian for charge neutral matter in equilibrium, which is called neutron star matter.

Once the solution has been found, the equation of state can be calculated from

$$\epsilon = \tfrac{1}{2} m_\sigma^2 \sigma^2 + \tfrac{1}{2} m_\omega^2 \omega_0^2 + \tfrac{1}{2} m_\rho^2 \rho_{03}^2 + \sum_B \frac{2J_B+1}{2\pi^2} \int_0^{k_B} \sqrt{k^2 + m_B^{*2}}\, k^2 dk + \sum_\lambda \frac{1}{\pi^2} \int_0^{k_\lambda} \sqrt{k^2 + m_\lambda^2}\, k^2 dk , \tag{17}$$

which is the energy density while the pressure is given by

$$p = -\tfrac{1}{2} m_\sigma^2 \sigma^2 + \tfrac{1}{2} m_\omega^2 \omega_0^2 + \tfrac{1}{2} m_\rho^2 \rho_{03}^2 + \tfrac{1}{3} \sum_B \frac{2J_B+1}{2\pi^2} \int_0^{k_B} k^4 dk / \sqrt{k^2 + m_B^{*2}} + \tfrac{1}{3} \sum_\lambda \frac{1}{\pi^2} \int_0^{k_\lambda} k^4 dk / \sqrt{k^2 + m_\lambda^2} . \tag{18}$$

The theory is simper to solve in the case of symmetric nuclear matter, and this is a necessary first step in determining the coupling constants from the saturation properties. For nuclear matter near saturation, we simply fix $k_n = k_p = k$. The scalar and vector coupling constants can then be fixed by the known saturation density ρ_0 and binding $B/A = (\epsilon/\rho)_0 - m_n$. The symmetry energy coefficient is

$$a_{\rm sym} = \frac{1}{2} \left[\frac{\partial^2(\epsilon/\rho)}{\partial t^2} \right]_{t=0} = \left[\frac{g_\rho}{m_\rho} \right]^2 \frac{k_0^3}{12\pi^2} + \frac{k_0^2}{6(k_0^2 + m^{*2})^{1/2}} , \quad t \equiv (\rho_n - \rho_p)/\rho , \tag{19}$$

and serves to fix the ρ coupling. In the above equation, k_0 denotes the Fermi momentum of symmetric nuclear matter at saturation, ρ_0. The coupling constants that yield the following properties of symmetric nuclear matter

$$\rho_0 = 0.16 \text{ fm}^{-3} , \quad B/A = -16.0 \text{ MeV} , \quad a_{\rm sym} = 32.5 \text{ MeV} , \quad K = 265 \text{ MeV} , \quad m_{\rm sat}^*/m = 0.796 \tag{20}$$

are

$$(g_\sigma/m_\sigma)^2 = 8.63 \text{ fm}^2 , \quad (g_\omega/m_\omega)^2 = 4.11 \text{ fm}^2 , \quad (g_\rho/m_\rho)^2 = 4.54 \text{ fm}^2 . \tag{21}$$

The first three properties determine the coupling constants, and the last two properties then follow automatically from the structure of he Lagrangian. It is remarkable that they are so close to the empirical values [12,13], although the effective mass is perhaps slightly too large [14].

For use later in discussing the Λ hyperon binding in nuclear matter, we note that the values of the scalar and vector field strengths at saturation are

$$S \equiv g_\sigma \sigma = 1.08\ \text{fm}^{-1}, \quad V \equiv g_\omega \omega_0 = 0.660\ \text{fm}^{-1}. \qquad (22)$$

The solution to the equations discussed above for neutron star matter, with hyperon to baryon coupling strength in accord with the Λ binding in nuclear matter (discussed in detail later in Sec. III A), $x_\rho = x_\sigma \equiv g_{H\sigma}/g_{N\sigma} = 0.7$, $x_\omega = 0.859$, which we adopt as a standard unless noted otherwise, is shown in Figs. 1 and 2. As we discuss later, these couplings are compatible with the Λ binding in nuclear matter, with hypernuclear levels, and moreover, are compatible with present knowledge of neutron star masses. The meson-field amplitudes and chemical potentials are shown in Fig. 1, and the particle populations (in lieu of Fermi momenta) are shown in Fig. 2, both as functions of baryon density. It is interesting to compare these with the fictional case that the only baryons are neutrons as in Fig. 3. In particular, notice that the electron chemical potential increases monotonically as a function of density, whereas, when the hyperons are taken into account, it saturates at about 200 MeV. It is also interesting to see how the composition of dense charge neutral matter is complex, as compared to the case where the hyperons are ignored. Even the neutron population is drastically altered, being little more populous than the proton or Λ at high density. The lepton populations are also drastically reduced by the hyperons because charge neutrality can be achieved among the baryons to high degree. This could have important affects on estimates of the transport properties of neutron star matter, in particular, the conductivity and the viscosity. These are vital properties that affect the stability to rotation by damping gravitation-radiation-reaction instabilities.

In Fig. 4, we show the equation of state for three cases:

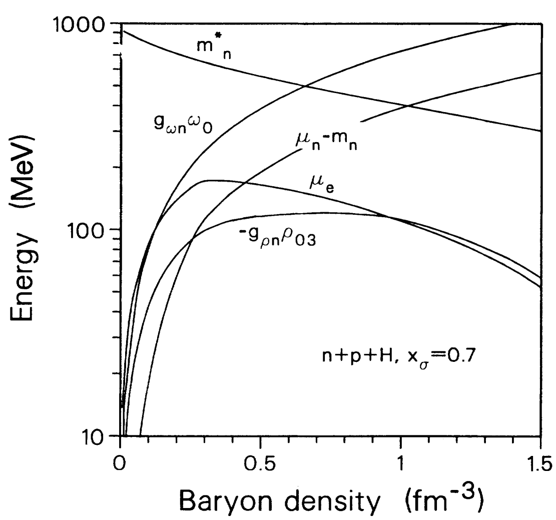

FIG. 1. Field amplitudes and chemical potentials that solve Eqs. (5)–(12) in the case of full equilibrium among all baryons to convergence. Hyperons are coupled as described in text. The Fermi momenta that constitute the rest of the solution are represented by the populations in Fig. 2.

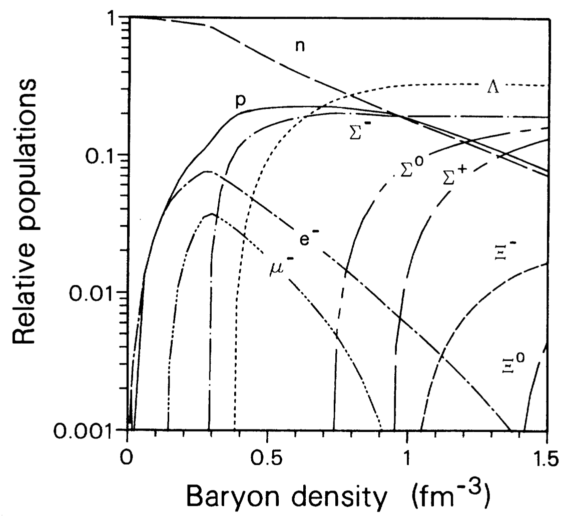

FIG. 2. Populations in neutron star matter as a function of density. Hyperon coupling as described in text is in accord with the Λ binding in nuclear matter.

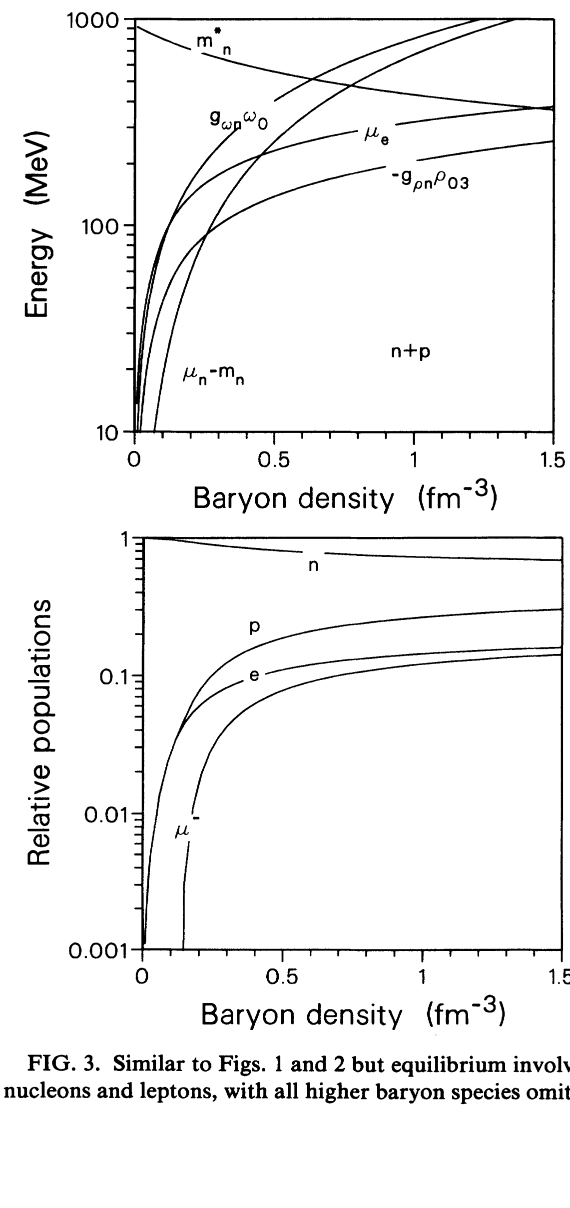

FIG. 3. Similar to Figs. 1 and 2 but equilibrium involves only nucleons and leptons, with all higher baryon species omitted.

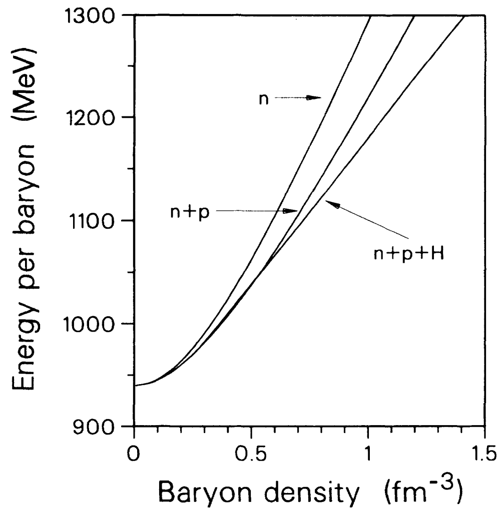

FIG. 4. Equation of state for three cases: n, only neutrons; $n+p$, nucleons in beta equilibrium with leptons; and $n+p+\text{H}$, nucleons and all other baryons to convergence, and all in equilibrium with leptons.

(1) pure neutron matter, (2) beta equilibrium between neutrons, protons, and leptons, and (3) equilibrium between all baryons to convergence and leptons. The hyperons of the third case are coupled as described following Eq. (22). It is evident that pure neutron matter is not the lowest-energy state of dense charge neutral matter and that the existence of hyperons considerably softens the equation of state, by relieving the Fermi pressure of the nucleons. In the last one, in actual fact, the baryon species populated to the highest densities in these neutron star models are the nucleons and hyperons of Table I with the exception of Ω whose mass is so large that it lies above the chemical potential. Δ is not populated for the same reasons given in Ref. [8], which can be understood in terms of the isospin symmetry of the nuclear forces acting within the absolute constraint of charge neutrality. Briefly, the most favored charge state, Δ^- is *isospin* unfavored by its large negative projection, $-\frac{3}{2}$ (same sign as the neutron), while the isospin-favored state, $+\frac{3}{2}$, Δ^{++}, is doubly *charge* unfavored (same sign as proton). The threshold condition can be read from Eq. (9),

$$\mu_n - q_B\mu_e \geq g_{\omega B}\omega_0 + g_{\rho B}\rho_{03}I_{3B} + m_B^* \tag{23}$$

and the field amplitudes appearing in it can be found in Fig. 1.

III. NEUTRON STAR STRUCTURE

The equations for the structure of a relativistic spherical and static star composed of a perfect fluid were derived from Einstein's equations by Oppenheimer and Volkoff [15]. They are

$$4\pi r^2 dp(r) = -\frac{M(r)dM(r)}{r^2}\left[1+\frac{p(r)}{\epsilon(r)}\right] \times\left[1+\frac{4\pi r^3 p(r)}{M(r)}\right]\left[1-\frac{2M(r)}{r}\right]^{-1}, \tag{24}$$

$$dM(r) = 4\pi r^2 \epsilon(r) dr\ . \tag{25}$$

(We use gravitational units, $G=c=1$.) Given an equation of state, they can be integrated from the origin as an initial value problem for a set of arbitrary choices of the central density. Therefore, they define a one-parameter family of stars. Corresponding to the three equations of state of Fig. 4, we show the three families of neutron stars in Fig. 5. The equation of state for the case of pure neutron matter lies above the other two because a pure neutron state is not the lowest-energy state of charge neutral matter. A state containing an equilibrium mixture of nucleons and leptons is lower and one containing an equilibrium population of all baryons to convergence is even lower. The latter two equations of state are coincident up to the threshold density of the first heavier baryon state beyond the nucleons. These features are also registered in the corresponding family of stars for the three cases.

The equations of star structure have to be integrated to the radius at which the pressure is zero, or very small compared to the central pressure. This means that the nuclear equation of state has to be supplemented by one corresponding to subnuclear densities. As described in Ref. [8], we use that of Negele and Vautherin [16] for the subnuclear region of very neutron rich nuclei, and of Harrison and Wheeler (17) for the lower-density crystalline lattice bathed in relativistic electrons.

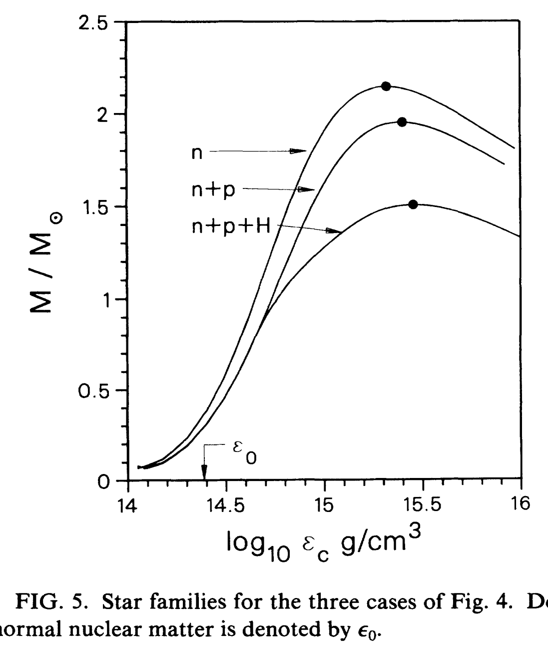

FIG. 5. Star families for the three cases of Fig. 4. Density of normal nuclear matter is denoted by ϵ_0.

A. Hyperon couplings: Constraints from hyperon binding in nuclei

The ratio of hyperon to nucleon couplings to the meson fields,

$$x_\sigma = g_{H\sigma}/g_\sigma, \quad x_\omega = g_{H\omega}/g_\omega, \quad x_\rho = g_{H\rho}/g_\rho, \tag{26}$$

are not defined by ground-state properties of nuclear matter and so must be chosen according to other considerations. (For brevity we call $g_{N,\sigma}$ simply g_σ.) In studies of hypernuclear levels [18–20], these ratios are typically taken to be equal. In that case, small values between 0.33 and 0.4 are required. These are too small as regards neutron star masses, as is shown in Fig. 6 and in Table II. Recall that the most accurately determined mass (but not necessarily the maximum possible mass) is the of PSR1913+16 with $M/M_\odot = 1.442 \pm 0.003$ [21]. There is another relevant measurement, that of 4U0900-40 with $M/M_\odot = 1.85^{+0.35}_{-0.3}$ [22]. However, the error is so large that many authors take the other measurement as the limit. The actual number of known masses at the present time is less than 10 and we cannot exclude that a more massive neutron star will be found. However, to the imperfect extent to which the type-II supernova mechanism is understood, it appears that neutron stars are created in a fairly narrow range of masses around, $\sim 1.4 M_\odot$, so that whether or not the true equation of state would support more massive neutron stars, none may be made in nature.

The hyperons are actually more *strongly* populated in dense neutron star matter, the equation of state correspondingly softened, and the limiting mass reduced, the *weaker* their coupling to the meson fields [4,6]. Indeed, even if the coupling is reduced to zero as for a Fermi gas model, but allowing the populations to reach equilibrium under the weak interactions, the hyperons are computed to be present in dense neutron star matter [23]. We can

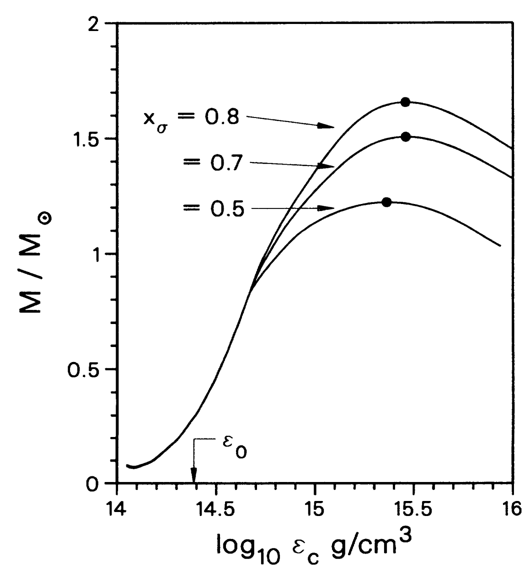

FIG. 6. Neutron star families for three values of the hyperon to nucleon coupling constants identified by x_σ. (See Table II.)

TABLE II. Values of the hyperon to nucleon scalar and vector coupling that are compatible with the binding of −28 MeV for lambda hyperons in nuclear matter and the corresponding maximum neutron star mass.

x_σ	x_ω	$M/M_\odot$
0.3	0.262	1.08
0.4	0.415	1.13
0.5	0.566	1.23
0.6	0.714	1.36
0.7	0.859	1.51
0.8	1.00	1.66
0.9	1.14	1.79
1.0	1.27	1.88

understand the increase of hyperon populations in dense matter with a decrease in their coupling relative to the nucleon since the high-density region is dominated by the repulsive interaction, so that the energy can be lowered by shifting baryon populations to hyperons. In the present theory the way it works is that, if the hyperon coupling is weaker than the nucleon, the vector field amplitude can be reduced by the shifting of the baryon populations in favor of those with the weaker coupling, as is clear from Eq. (5). This, in turn, lowers the energy by reducing the repulsive vector contribution, $\frac{1}{2} m_\omega^2 \omega_0^2$, in Eq. (17): weakening the coupling in dense matter amounts therefore to weakening the repulsion.

As noted above, when hypernuclear levels are analyzed with the constraint $x_\sigma = x_\omega$, the result is a small hyperon coupling leading to a neutron star family with much too small a limiting mass. However, one is not compelled to take the ratios in Eq. (26) to be equal, but there are large correlation errors in $x_\sigma = 0.464 \pm 0.255$, $x_\omega = 0.481 \pm 0.315$, in the published analysis of hypernuclear levels that leave them uncorrelated [20]. These correlation errors are probably due to the degeneracy with respect to the Λ binding in nuclear matter which we derive next. As noted elsewhere [24], this binding energy serves to strictly correlate the values of x_σ, x_ω, but leaves a continuous pairwise ambiguity which hypernuclear levels may be able to resolve. The published analysis so far does not take account of this [20]. In Ref. [25], the binding of the Λ hyperon in nuclear matter is inferred to be −28 MeV. We derive now the expression for this binding in our model. From the Weisskopf [26] relation at saturation between the Fermi energy and the energy per nucleon of a self-bound system, $e_F = (\epsilon/\rho)_0$, which is a special case of the Hugenholtz–Van Hove theorem [27], we obtain for the binding energy of the lowest Λ level in nuclear matter

$$\left[\frac{B}{A}\right]_\Lambda = x_\omega V + m_\Lambda^* - m_\Lambda$$

$$= x_\omega V - \frac{x_\sigma S}{1 + x_\sigma S/2m_\Lambda}, \tag{27}$$

where S, V were defined and their values given in Eq. (22) and we have used Eqs. (4) and (16). The first line holds for both the linear and nonlinear σ-ω theories as well as this one. The second line specializes to this one. Thus, as far as the Λ binding in nuclear matter is concerned, the scalar and vector ratios x_σ, x_ω need not be equal, but when so, they must be small, about 0.37. We show a few typical values in Table II and also in Fig. 6. Since the neutron star mass limit must exceed about $(1.44-1.5)M_\odot$, and as it depends on the hyperon coupling, we infer that $x_\sigma > 0.65$ and corresponding value of x_ω, as given by Eq. (27). There are additional constraints that can be invoked. There is good reason to believe [28] that these ratios are less than unity. Moreover, according to the analysis of hypernuclear levels in finite nuclei, it is found that when the ratios are taken unequal, the maximum likely value is $x_\sigma < 0.719$ [20]. It is not clear how strong this last constraint is because it applies to the nonlinear field theory [3] whose results would carry over only approximately to the present one. For such relatively simple theories of matter, perhaps one should not insist that when the interest is focused on bulk matter, the level spacings of finite nuclei are compelling constraints. In any case, for x_σ, x_ω chosen to be compatible with the Λ binding in nuclear matter, neutron star masses place a lower bound on the coupling, and hypernuclear levels appear to place an upper bound, but so far less well determined. Within this range, as we shall see in the next section, hyperons have a large population in neutron stars and neutrons have a bare majority.

We have assumed that other hyperons in the lowest octet have the same coupling as the Λ, and also we have arbitrarily taken $x_\rho = x_\sigma$. This choice produces results very close to another possible one, $x_\rho = x_\omega$.

We add here a parenthetical note on the analysis of hypernuclei, involving both the Λ or any other hyperon. We quoted above the $\sim 50\%$ correlation error found in the least-squares fit of x_σ, x_ω to the hypernuclear levels when the parameters are treated independently [20]. But these are not independent parameters as we derived above. They are correlated in a specific way to the binding of the Λ in saturated nuclear matter, a binding that can be inferred quite accurately by an extrapolation from hypernuclear levels in finite A nuclei [25]. The correlation found in the least-squares fit is simply a reflection of the fact that, as a function of A, the finite nuclei are "pointing" to this binding in $A \to \infty$ matter. It is clear, therefore, that it would be advantageous in the analysis of hypernuclei to take into account the relation that x_σ, x_ω must obey, if the Λ binding in nuclear matter is to come out right. In the linear [2] and nonlinear scalar [3] versions of nuclear field theory, the difference in masses entering the first line of Eq (27) is $m_H^* - m_H = -x_\sigma S$, whereas in the present hybrid derivative coupling model it is given by the second line of Eq. (27).

B. Baryon populations

Since we have a covariant theory that accounts rather well for the ground-state properties of nuclear matter and for which the hyperon couplings are constrained by the following data, (1) neutron stars of mass at least $1.442 M_\odot$ exist, (2) the Λ binding in saturated nuclear matter, and (3) hypernuclear levels in finite nuclei, we now note the predicted hyperon populations in neutron stars. The populations of the maximum-mass star of $1.51 M_\odot$ corresponding to the coupling $x_\sigma = 0.7$ of Table II, as a function of radius, are shown in Fig. 7 for the case of full equilibrium of all baryons. This coupling falls in the small acceptable range. Although the neutron is the largest of the populations, it has a bare majority. The core itself is dominated by hyperons. Integrated over the whole star, the hyperons amount to 29% of the baryon population in this maximum-mass model, the neutrons to 54%, and the protons to 17%. Nevertheless, the hyperons alter drastically the interior, up to a radius of 6–7 km, shifting negative charge from leptons to hyperons as can be seen by comparison with Fig. 8. This will certainly affect the electrical conductivity of the star, which is relevant to the decay rate of the magnetic field of pulsars.

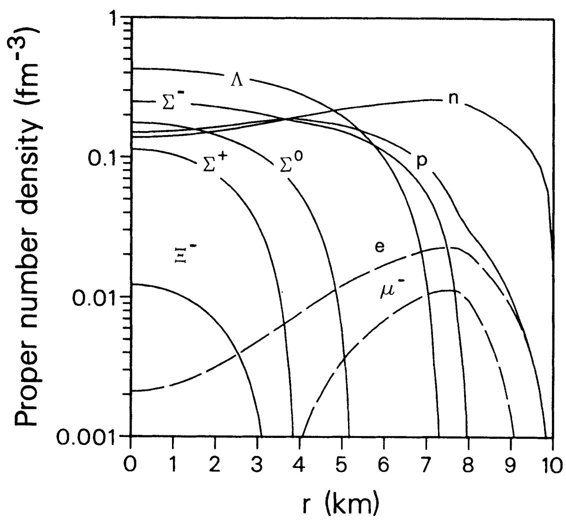

FIG. 7. Populations in the maximum mass star for case $x_\sigma = 0.7$ in Fig. 6. Central baryon density is 1.28 fm^{-3}.

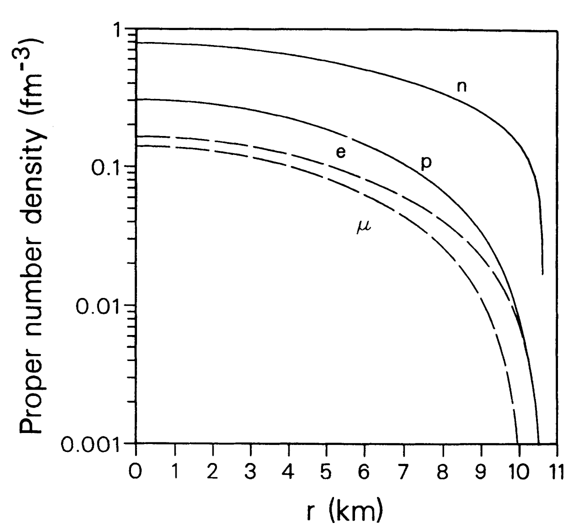

FIG. 8. Populations in the maximum mass star corresponding to $n+p$ in Fig. 5. Central baryon density is 1.1 fm^{-3}.

We have already noted in connection with Fig. 5 that the hyperons reduce the limiting neutron star mass under what would be calculated in a pure neutron approximation by about $\frac{3}{4}M_{\odot}$ and by about $\frac{1}{2}M_{\odot}$ under the case that beta equilibrium only with respect to nucleons and leptons is accounted for.

C. Mass-radius relation, Kepler frequency, moment of inertia

The mass-radius relation is an important one because it can be used to estimate how rapidly the stars in the family belonging to a given equation of state can rotate without shedding mass at the equator. Such relations for the three cases of Fig. 6 are shown in Fig. 9. The curves marked in m are such that stars falling below a given curve can rotate without mass loss to at least the period marked on the curve. These periods correspond to the relativistic Kepler frequency of the limiting mass star in the sequence belonging to an equation of state, and can be approximated [29,30] by

$$\Omega_K \approx 0.65\Omega_c \ ,$$
$$\Omega_c = \sqrt{M/R^3} = 3.7\times 10^5 \left[\frac{M/M_{\odot}}{(R/\mathrm{km})^3} \right]^{1/2} \mathrm{s}^{-1} \ , \tag{28}$$

where Ω_c is the Newtonian Kepler frequency at which centrifuge and gravity balance. The factor 0.65 is empirical, approximate, and is particular to typical limiting-mass neutron star models, and has its origin in the general relativistic dragging of the local inertial frame [31], the centrifugal effects being determined by the difference in the angular velocity of the star and the angular velocity of the local inertial frames [32]. We see from the figure that some stars in all these families can rotate at 1.5 ms but none at 0.5 ms so far as the limitation of mass loss at the equator is concerned.

We have also carried out a general relativistic calculation of the Kepler frequency using the Hartle-Thorne perturbative method of solving the equations for rotating stellar structure [33,32]. When this method is supplemented by a self-consistency condition on the frequency that was first introduced into the method in Ref. [34], the perturbative method is found to be in accord with an exact numerical calculation of Einstein's equations, as shown in Ref. [31], up to the highest frequency that neutron stars, limited by gravity-wave instabilities, can have [35].

The ingredient missing from earlier applications of Hartle's method is the transcendental equation for the general relativistic Kepler frequency. It is given by [36]

$$\Omega_K = e^{\nu-\psi}V(\Omega_K) + \omega(\Omega_K) \ , \tag{29}$$

$$V(\Omega_K) \equiv \frac{\omega'}{2\psi'}e^{\psi-\nu} + \left[\frac{\nu'}{\psi'} + \left[\frac{\omega'}{2\psi'}e^{\psi-\nu} \right]^2 \right]^{1/2} . \tag{30}$$

Equations (29) and (30) are to be evaluated at the star's equator. The quantity V denotes the orbital velocity measured by an observer with zero angular momentum in the ϕ direction. Primes refer to derivatives with respect to the radial coordinate. The quantity ω denotes the frequency of the local inertial frame (dragging effect). An essential feature is that V and ω (like the metric functions ν and ψ) depend on Ω_K. Therefore, to find the Kepler frequency, a self-consistent solution of Hartle's equations that satisfies the above transcendental relation for Ω_K must be constructed. Details of how this can be done are given in Ref. [34].

We show the relativistic Kepler frequency for the sequence of stars belonging to $x \equiv x_\sigma = x_\omega = x_\rho = 0.82$ in Fig. 10 and compare it with the classical result Ω_c of Eq. (28). (This representative case differs from the case $x_\sigma = 0.7$, $x_\omega = 0.859$ of Table I, by $<0.02\%$ in mass and

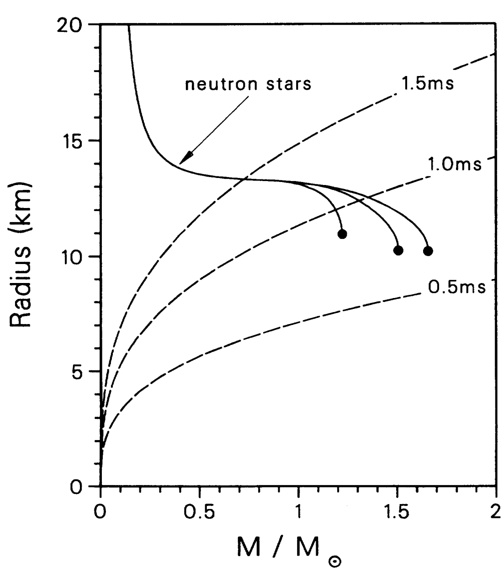

FIG. 9. Mass-radius relation for the same star families as in Fig. 6.

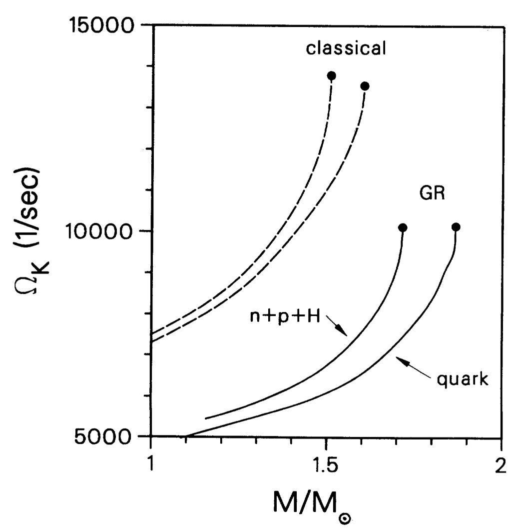

FIG. 10. Kepler angular velocity in classical and general relativity physics for two sequences of stars, a neutron star, $(n+p+\mathrm{H})$, and quark hybrid star.

radius over the whole family.) The relativistic frequency is lower than the classical one because of the phenomenon in general relativity know as dragging of the local inertial frame by the rotation of the star, and because of centrifugal flattening of the star, the two effects contributing about equally [31]. While unimportant in most stars, frame dragging becomes significant in rapidly rotating neutron stars. The centrifugal effects are given by the excess of the rotational frequency of the star over the (radially dependent) frame dragging frequency. Also shown in the figure is the case discussed in the next section in which the core of the star is in the mixed phase of hadronic and quark matter. This figure also shows how the limiting mass of a sequence belonging to a particular equation of state is increased by rotation at the Kepler frequency, from $1.5M_\odot$ to $1.7M_\odot$, in the case of the star at the limit.

It is relevant to note that the shortest period so far observed is 1.6 ms for PSR1937+21, discovered in 1982 [37]. It is clear that this period poses no constraint on the theory of matter when the shortest period is estimated as the Kepler (mass shedding) period. We will later discuss gravitational-radiation instabilities that limit the shortness of the period of rotation even more severely than mass shedding.

The moment of inertia in general relativity is given by

$$I=\frac{8\pi}{3}\int_0^R dr\, r^4 \frac{\epsilon(r)+p(r)}{\sqrt{1-2m(r)/r}}e^{-\phi(r)}\frac{\Omega-\omega(r)}{\Omega}\ , \qquad (31)$$

where $\omega(r)$ is the angular velocity of the local inertial frame (frame dragging), and for slow rotation is much smaller than the stars angular velocity, Ω. We therefore neglect it in the calculation of I. The function $\Phi(r)$ is related to the metric function $g_{00}=e^{2\Phi}$ and is the solution of

$$\frac{d\Phi}{dr}=\frac{m(r)+4\pi r^3 p(r)}{r[r-2m(r)]}\ , \qquad (32)$$

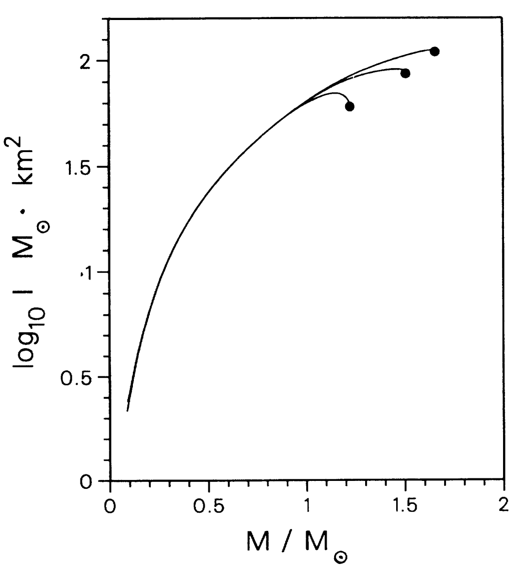

FIG. 11. Moment of inertia, I, for the same star families as in Fig. 6.

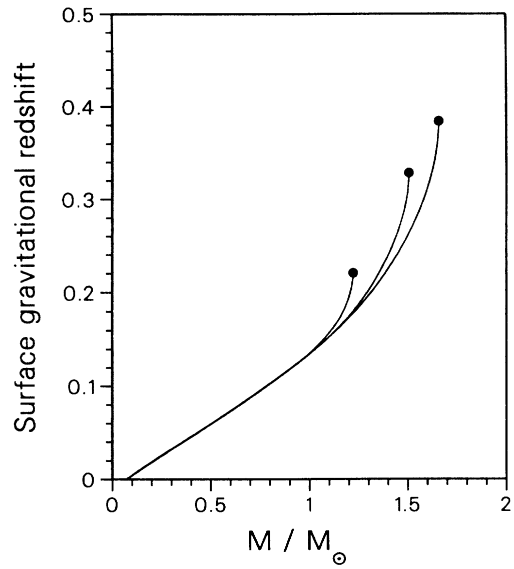

FIG. 12. Surface redshift as a function of neutron star mass for the same families as in Fig. 6.

with boundary condition

$$2\Phi(R)=\ln\left[1-\frac{2M}{R}\right]\ , \qquad (33)$$

where M,R are the star's mass and radius. For the three couplings of hyperons of Fig. 6, we show the moment of inertia in Fig. 11. Little is known about the moments of inertia of neutron stars. However, assuming, as is likely, that the energy required to power the crab nebula, about 4×10^{38} erg s^{-1}, is provided by the loss of rotational energy by the pulsar, its moment of inertia is at least $40M_\odot$ km^2 [38]. This can be accounted for by all of the couplings shown in this figure.

There is a constraint relating the mass and surface redshift as determined from gamma-ray bursters. It is, at present, a very weak constraint because the redshift is not measured for any neutron star whose mass is also known. All we know is that the surface redshifts seem to lie in the range $z\equiv\Delta\lambda/\lambda=0.2-0.5$ [39] while masses seem to lie in the range $M/M_\odot=1-1.85$ with an error of ±0.3 at both ends [22]. In any case, eventually a redshift for a star whose mass is also known may be measured, so we show in Fig. 12 the surface redshift,

$$z=1/\sqrt{1-2M/R}-1\ , \qquad (34)$$

as a function of mass.

IV. GRAVITATIONAL-RADIATION-REACTION INSTABILITY

The Kepler frequency, above which centrifuge overwhelms gravity at the equator of a rotating star, provides only an absolute upper bound on frequency. There is another instability that sets in at lower frequency which therefore provides a more stringent and realistic limit [40]. It originates in counter-rotating surface vibrational modes, which at sufficiently high rotational frequency of the star are dragged forward. In this case, gravitational radiation, which inevitably must accompany the aspherical transport of matter, does not damp the modes, but rather drives them [41,42]. Viscosity plays the important role of damping such gravitational-wave–driven instabilities at a sufficiently reduced frequency such that the viscous damping rate and power in gravity waves are comparable [43]. We have found recently that these viscosity modified gravitational-radiation instabilities may set in at a significantly small fraction (60–70 %) of the Kepler frequency and therefore set a more realistic upper bound than the latter [34,35].

Of course, the normal modes of a star corresponding to a specific equation of state are numerically very difficult to obtain, and approximation schemes based on Maclaurin spheroids have been developed. The modes are taken to have the dependence $\exp[i\omega_m(\Omega)t+im\phi-t/\tau_m(\Omega)]$, where ω_m is the frequency of the $m=l$ surface mode which also depends on the angular velocity, Ω of the star, ϕ is the azimuthal angle, and τ_m is the time scale for the mode which determines its growth or damping. The rotation frequency Ω at which it changes sign is the critical frequency for the particular mode, m. It is conveniently expressed as the frequency, Ω_m, that solves [40]

$$\Omega_m=\frac{\omega_m(0)}{m}\left[\alpha_m(\Omega_m)+\gamma_m(\Omega_m)\left[\frac{\tau_{G,m}}{\tau_{V,m}}\right]^{1/(2m+1)}\right] . \tag{35}$$

In this equation, the frequency of the vibrational mode in a nonrotating star is given by [44]

$$\omega_m(0)=\Omega_c\left[\frac{2m(m-1)}{2m+1}\right]^{1/2} , \tag{36}$$

where Ω_c was given in Eq. (28). The time scale for gravitational radiation reaction is [45]

$$\tau_{G,m}=\frac{2}{3}\frac{2(m-1)[(2m+1)!!]^2}{(m+1)(m+2)}\left[\frac{2m+1}{2m(m-1)}\right]^m \times\Omega_c^{-2(m+1)}R^{-(2m+1)} , \tag{37}$$

and that for viscous damping is [46]

$$\tau_{V,m}=\frac{R^2}{(2m+1)(m-1)}\frac{\bar{\rho}}{\eta} , \tag{38}$$

where $\bar{\rho}=M/(\frac{4}{3}\pi R^3)$. The shear viscosity is denoted by η and depends on the temperature of the star, being small in very hot and therefore young stars and larger in cold stars. The functions α_m and γ_m contain information about the pulsation of the rotating star models and are difficult to determine [40,47]. However, it turns out that they are rather weakly dependent on the equation of state and are close to unity and have sometimes been approximated as such. Here we take $\alpha_m(\Omega_m)$ and $\gamma_m(\Omega_m)$ as calculated in Refs. [48,49] (for the oscillations of rapidly rotating inhomogeneous Newtonian stellar models; polytropic index $n=1$) and Ref. [40] (for uniform-density Maclaurin spheroids, i.e., $n=0$, respectively. In the above approximation scheme, the properties of the particular model star enter through its mass and radius which occurs in the above equations, not on other details of the equation of state except insofar as it determines these quantities. Indeed, in a study of polytropes, it has been confirmed that Ω_m depends much more strongly on the radius and mass of the neutron star model (through Ω_c, $\tau_{V,m}$, and $\tau_{G,m}$) than on the polytropic index assumed in calculating α_m [50].

To relate the temperature and viscosity of a star, we adopt the expression [51,47]

$$\eta=347\bar{\rho}^{9/4}/T^2 , \tag{39}$$

where $\bar{\rho}$ is the density in g/cm^3, T is temperature in K, and η is the shear viscosity in g/(cm s). Bulk viscosity has a different temperature dependence [52] and may be important at high temperature before it falls below $T\sim10^{11}$ K in a newly born star. If so, then the minimum stable period of a hot star could be less than our estimate.

In Fig. 13 is shown the minimum stable period that the family of neutron stars corresponding to hyperon coupling $x=0.82$ can have in the face of viscosity moderated gravitation-reaction instabilities. It is a very strong function of the mass and radius of the star. The minimum stable period of a hot star establishes the limit of the star during its lifetime so long as it is isolated and remains so. (The presence of a binary companion is easily detected in the frequency modulation of the pulses of a pulsar.) For the limiting-mass star, the minimum period is about 1 ms. It is a strong function of the mass of the star, through the dependence on radius. For comparison, from Fig. 10, the Kepler period of the limiting mass star is $P\sim0.63$ ms (and similarly for the hybrid star). So the gravity-wave instabilities set a much more stringent limit on stable rotation than the mass shedding limit for stars whose histo-

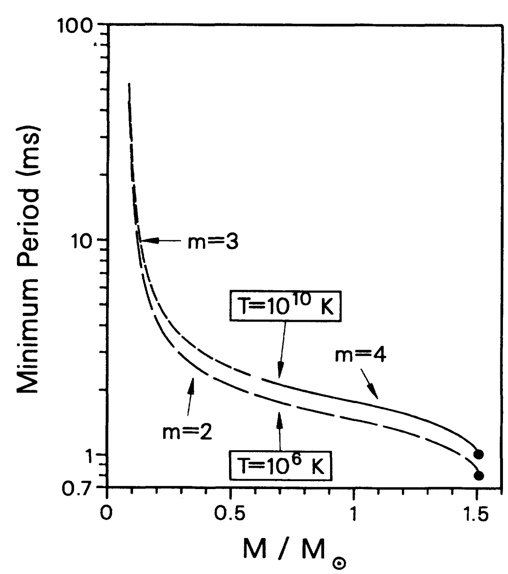

FIG. 13. Minimum period that is stable against gravitational-radiation-reaction for hot and cold stars for a family of neutron stars. See also discussion of Fig. 10.

ry has left them isolated from a companion. The $T=10^6$ K curve of Fig. 13 is relevant to old cold stars that have acquired a companion, and spin up by accretion. In this case, gravitational-radiation instability is closer to the Kepler mass-shedding instability.

V. SUMMARY

We have computed a large number of neutron star properties, perhaps more than has been computed for any other single model. In this case the model corresponds to the derivative coupling Lagrangian involving the exchange of scalar, vector, and vector-isovector mesons. It describes quite accurately the five bulk properties of symmetric nuclear matter in the mean-field approximation. For the description of charge neutral equilibrium matter (neutron star matter), we include all baryon states to convergence at the highest densities appearing in the corresponding neutron star models. These turn out to be nucleons and hyperons, but not deltas. Several different hyperon couplings were employed. The dependence is similar to that found in Refs. [8,4,6], namely, the smaller the hyperon to nucleon coupling, the more strongly the hyperons contribute. This seemingly inverted behavior actually is a logical consequence of the fact that the high-density equation of state is dominated by the repulsion of the vector mesons. There is a small range in which hyperon couplings are compatible with bounds place by (1) observed neutron star masses, (2) the binding of the Λ hyperon in saturated nuclear matter, and (3) hypernuclear levels, which, in the published literature, provide a weaker constraint than the foregoing. In this range, hyperons are a large population in $1.5M_\odot$ neutron stars and neutrons are a bare majority population. It is clear that the mass limit computed for neutron stars is sensitive to the presence of hyperons with coupling so chosen to agree with the above constraints and it is substantially below the value that would be obtained with their neglect, by about $\frac{1}{2}M_\odot$ compared to a model in which beta equilibrium only between nucleons and leptons is allowed for.

We also computed the minimum rotational period imposed by gravitational-radiation-reaction instabilities, which is appreciably larger than the Kepler period, and therefore sets the minimum rotational period of neutron star models. According to our finding here and earlier [34,35], the gravitational-wave instability effectively limits the period of neutron stars to $P>1$ ms unless, as cold stars, they have been spun up by accretion. Then the period can be slightly smaller. The period of the fastest pulsar known so far [37] with $P=1.56$ ms is easily accommodated by the theory of dense matter discussed here whether or not a phase transition to quark matter has occurred.

ACKNOWLEDGMENTS

This work was supported by the Division of Nuclear Physics, of the U.S. Department of Energy under Contract No. DE-AC03-76SF00098. One of us (F.W.) acknowledges financial support from the Max Kade Foundation.

[1] J. Zimanyi and S. A. Moszkowski, Phys. Rev. C **42**, 1416 (1990).

[2] M. H. Johnson and E. Teller, Phys. Rev. **98**, 783 (1955); H. P. Duerr, *ibid.* **103**, 469 (1956); J. D. Walecka, Ann Phys. **83**, 491 (1974).

[3] J. Boguta and A. R. Bodmer, Nucl. Phys. **A292**, 413 (1977).

[4] N. K. Glendenning, Nucl. Phys. **A493**, 521 (1989).

[5] J. I. Kapusta and K. A. Olive, Phys. Rev. Lett. **64**, 13 (1990).

[6] J. Ellis, J. I Kapusta, and K. A. Olive, Nucl. Phys. **B348**, 345 (1991).

[7] S. I. A. Garpman, N. K. Glendenning, and Y. J. Karant, Nucl. Phys. **A322**, 382 (1979).

[8] N. K. Glendenning, Astrophys. J. **293**, 470 (1985).

[9] N. K. Glendenning, B. Banerjee, and M. Gyulassy, Ann. Phys. (N.Y.) **149**, 1 (1983).

[10] J. D. Bjorken and S. D. Drell, *Relativistic Fields* (McGraw-Hill, New York, 1965).

[11] B. D. Serot and J. D. Walecka, in *Advances in Nuclear Physics,* edited by J. W. Negele and E. Vogt (Plenum, New York, 1986).

[12] N. K. Glendenning, Phys. Rev. C **37**, 2733 (1988).

[13] M. M. Sharma, W. T. A. Borghols, S. Brandenburg, S. Crona, A. van der Woude, and M. N. Harakeh, Phys. Rev. C **38**, 2562 (1988).

[14] M. Jaminon and C. Mahaux, Phys. Rev. C **40**, 354 (1989).

[15] J. R. Oppenheimer and G. M. Volkoff, Phys. Rev. **55**, 374 (1939).

[16] J. W. Negele and D. Vautherin, Nucl. Phys. **A178**, 123 (1973).

[17] B. K. Harrison, K. S. Thorne, M. Wakano, and J. A. Wheeler, *Gravitation Theory and Gravitational Collapse* (University of Chicago, Chicago, 1965).

[18] J. Boguta and S. Bohrmann, Phys. Lett. **102B**, 93 (1981).

[19] G. E. Walker, Nucl. Phys. **A450**, 287c (1986).

[20] M. Rufa, J. Schaffner, J. Marhun, H. Stocker, W. Greiner, and P.-G. Reinhard, Phys. Rev. C **42**, 2469 (1990).

[21] J. H. Taylor and J. M. Weisberg, Astrophys. J. **345**, 434 (1989).

[22] P. C. Joss and S. A. Rappaport, Annu. Rev. Astron. Astrophys. **22**, 537 (1984).

[23] V. A. Ambartsumyan and G. S. Saakyan, Astron. Zh. **37**, 193 (1963) [Sov. Ast. AJ **4**, 187 (1960)].

[24] N. K. Glendenning and S. A. Moszkowski, Phys. Rev. Lett. **67**, 2414 (1991).

[25] D. J. Millener, C. B. Dover, and A. Gal, Phys. Rev. C **38**, 2700 (1988).

[26] V. F. Weisskopf, Rev. Mod. Phys. **29**, 174 (1957).

[27] N. M. Hugenholtz and L. Van Hove, Physica **24**, 363 (1958).

[28] S. A. Moszkowski, Phys. Rev. D **9**, 1613 (1974).

[29] J. L. Friedman, J. R. Ipser, and L. Parker, Phys. Rev. Lett. **62**, 3015 (1989).

[30] P. Haensel and J. L. Zdunik, Nature **340**, 617 (1989).

[31] F. Weber and N. K. Glendenning, Astrophys. J. (in press).

[32] J. B. Hartle and K. S. Thorne, Astrophys. J. **153**, 807 (1968).
[33] J. B. Hartle, Astrophys. J. **150**, 1005 (1967).
[34] F. Weber, N. K. Glendenning, and M. K. Weigel, Astrophys. J. **373**, 579 (1991).
[35] F. Weber and N. K. Glendenning, Z. Phys. A **339**, 211 (1991).
[36] J. L. Friedman, J. R. Ipser, and L. Parker, Astrophys. J. **304**, 115 (1986).
[37] D. C. Backer, S. Kulkarni, C. Heiles, M. M. Davis, and W. M. Goss, Nature **300**, 615 (1982).
[38] R. N. Manchester and J. H. Taylor, *Pulsars* (Freeman, San Francisco, 1977).
[39] E. P. Liang, Astrophys. J. **304**, 682 (1986).
[40] L. Lindblom, Astrophys. J. **303**, 303 (1986).
[41] S. Chandrasekhar, Phys. Rev. Lett. **24**, 611 (1970).
[42] J. L. Freidman, Phys. Rev. Lett. **51**, 11 (1983).
[43] L. Lindblom and S. L. Detweiler, Astrophys. J. **211**, 565 (1977).
[44] W. Thomson, Philos. Trans. R. Soc. London **153**, 608 (1863).
[45] S. L. Detweiler, Astrophys. J. **197**, 203 (1975).
[46] H. Lamb, Proc. London Math. Soc. **13**, 51 (1881).
[47] C. Cutler and L. Lindblom, Astrophys. J. **314**, 234 (1987).
[48] J. R. Ipser and L. Lindblom, Phys. Rev. Lett. **62**, 2777 (1989).
[49] J. R. Ipser and L. Lindblom, Astrophys. J. **355**, 226 (1990).
[50] R. A. Managan, Astrophys. J. **309**, 598 (1986).
[51] E. Flowers and N. Itoh, Astrophys. J. **206**, 218 (1976).
[52] R. F. Sawyer, Phys. Lett. **233**, 412 (1989).